PHYSICS

F. R. Verdun
A. Noel
R. Meuli
M. Pachoud
P. Monnin
J.-F. Valley
P. Schnyder
A. Denys

Influence of detector collimation on SNR in four different MDCT scanners using a reconstructed slice thickness of 5 mm

F. R. Verdun (✉) · M. Pachoud
P. Monnin · J.-F. Valley
University Institute
for Applied Radiophysics,
Grand-Pré 1, 1007 Lausanne, Switzerland
e-mail: francis.verdun@hospvd.ch
Tel.: +41-21-6233434
Fax: +41-21-6233435

A. Noel
Medical Physics Division,
A. Vautrin Centre (CAV),
54500 Vandoeuvre-lès-Nancy, France

R. Meuli · P. Schnyder · A. Denys
Department of Diagnostic
and Interventional Radiology,
University Hospital Centre (CHUV),
1011 Lausanne, Switzerland

Abstract The purpose of this paper is to compare the influence of detector collimation on the signal-to-noise ratio (SNR) for a 5.0 mm reconstructed slice thickness for four multi-detector row CT (MDCT) units. SNRs were measured on Catphan test phantom images from four MDCT units: a GE LightSpeed QX/I, a Marconi MX 8000, a Toshiba Aquilion and a Siemens Volume Zoom. Five-millimetre-thick reconstructed slices were obtained from acquisitions performed using detector collimations of 2.0–2.5 mm and 5.0 mm, 120 kV, a 360° tube rotation time of 0.5 s, a wide range of mA and pitch values in the range of 0.75–0.85 and 1.25–1.5. For each set of acquisition parameters, a Wiener spectrum was also calculated. Statistical differences in SNR for the different acquisition parameters were evaluated using a Student's t-test ($P<0.05$). The influence of detector collimation on the SNR for a 5.0-mm reconstructed slice thickness is different for different MDCT scanners. At pitch values lower than unity, the use of a small detector collimation to produce 5.0-mm thick slices is beneficial for one unit and detrimental for another. At pitch values higher than unity, using a small detector collimation is beneficial for two units. One manufacturer uses different reconstruction filters when switching from a 2.5- to a 5.0-mm detector collimation. For a comparable reconstructed slice thickness, using a smaller detector collimation does not always reduce image noise. Thus, the impact of the detector collimation on image noise should be determined by standard deviation calculations, and also by assessing the power spectra of the noise.

Keywords CT · Dose reduction · Dosimetry · Image quality · Optimization

Introduction

To increase volume coverage in a shorter time while maintaining an excellent longitudinal resolution, manufacturers have developed multi-detector row CT scanners (MDCT). Compared with single-slice CT units, MDCT scanners have arrays of detectors that can simultaneously acquire several slices per 360° X-ray tube rotation. With these systems, the smallest slice thickness that can be obtained is equal to the length, in the longitudinal direction, of the smallest detector cell—referred to here as the detector collimation. At the end of the data acquisition, z-filtering algorithms can be used to vary the reconstructed slice thickness from the detector collimation thickness to up to 10 mm. Thus, data acquired with a detector collimation of 2.0 mm can be reconstructed as 5.0-mm-thick slices.

The use of a smaller detector collimation than the reconstructed slice thickness has several advantages. For example, it permits the reconstruction of low-artefact sagittal or coronal slices, and also the reconstruction at some later time after the data acquisition, of slices with a thick-

ness equal to or close to the detector collimation, should a higher longitudinal resolution be required [1–10].

The goal of this study is to investigate for four different MDCT units the effect of using a 2.0–2.5-mm detector collimation (compared with a 5-mm detector collimation) on the image noise level for 5.0-mm-thick reconstructed slices, at equivalent dose levels.

Materials and methods

Data acquisition

Images were acquired on four MDCT scanners: (A) a GE LightSpeed QX/i (GE Medical Systems, Milwaukee, WI), (B) a Marconi MX 8000 (Philips Medical Systems, Best, The Netherlands), (C) a Toshiba Aquilion (Toshiba Medical Systems Europe, Zoetermeer, The Netherlands) and (D) a Siemens VZ (Volume Zoom, Siemens Medical Systems, Erlangen Germany). The GE scanner has 16 rows of 1.25-mm-wide detectors; the Marconi and Siemens scanners have two rows each of 1-, 1.5-, 2.5- and 5-mm wide detectors (eight rows total), and the Toshiba has four rows of 0.5-mm- and 30 rows of 1-mm-wide detectors.

Acquisitions were performed at 120 kV, using a 360° gantry rotation time of 0.5 s, and a wide range of tube currents (100–400 mA). On units A and D, acquisitions were performed using detector collimations of 2.5 and 5.0 mm with pitch values of 0.75 and 1.5. On unit B, acquisitions were performed using detector collimations of 2.5 and 5.0 mm with pitch values of 0.875 and 1.25 (because pitch values of 0.75 and 1.5 were not available on this system). On unit C, acquisitions were performed using detector collimations of 2.0 mm and 5.0 mm with pitch values of 0.75 and 1.5. Acquisitions were repeated three times for each set of acquisition parameters to improve the statistics of the results. The manufacturer-recommended reconstruction filter for standard abdominal acquisitions was used, and the field of view (FOV) was set to 36 cm.

Dosimetry

All units displayed the $CTDI_w$ and the DLP corresponding to the acquisition protocol. These data were verified by measuring the $nCTDI_{100,w}$ using a 32-cm-diameter CTDI test object and a 10-cm-long CT pencil ionisation chamber connected to an electrometer (Radcal 1035-10.3 CTDI chamber and MDH 1015 electrometer, Radcal, Monrovia, CA). The ion chamber and electrometer were calibrated in RQR9 and RQA9 beams according to IEC 61267 [11], and traceable to the Swiss Federal Office of Metrology. For each set of acquisition parameters, the volume CTDI ($CTDI_{vol}$) was calculated by dividing the $CTDI_w$ by the pitch value, according to its definition [12, 13].

Image quality assessment

Signal-to-noise ratio (SNR) was assessed for images of the commercially available Catphan 500 CT phantom (The Phantom Lab-

oratory, Cambridge, NY), with the additional ring provided by the manufacturer to simulate the absorption of a standard abdomen in place. With the additional ring in place, the total diameter of the test phantom is 30 cm. The SNR was calculated in a homogeneous area of about 1,500 pixels at the centre of the FOV, by dividing the average pixel value (close to 55 HU for all the CT units) by the standard deviation of the pixel values. The SNR was evaluated on each of the three exposures made with the same acquisition parameters, and an averaged SNR was calculated. For each scanner, a Student's t-test ($P<0.05$) was used to evaluate the statistical differences in SNR between the different acquisition parameters.

To characterize the spatial frequency content of the image noise, a Wiener spectrum (i.e., a noise power spectrum dividing the noise variance into spatial frequencies) was calculated for the images obtained with a tube current of 300 mA. In each image, a homogeneous area of 128×128 pixels was divided into four 64×64 pixel subregions, and the Wiener spectrum was calculated for each subregion [13]. An averaged Wiener spectrum was calculated for each combination of pitch value and detector collimation (four Wiener spectra per image and three images for each set of acquisition parameters).

For each scanner and combination of pitch value and detector collimation, the full-width at half maximum (FWHM) of the slice sensitivity profile (SSP) was assessed using a bead point source in the CPT528 module of the Catphan 500 test phantom. The CPT528 module was scanned in the test object, and the SSP values were obtained by plotting a profile through the bead in a sagittal reconstruction, as recommended by the manufacturer.

Results

Table 1 shows the normalised weighted CTDI ($nCTDI_w$) measured at 120 kV in the 32 cm CTDI test phantom. There is good agreement between the scanner displays and the measured values ($\pm10\%$).

Figures 1a, 2a and 3a (for units A, B and C, respectively) show the variation in SNR as a function of $CTDI_{vol}$, for a nominal reconstructed slice thickness of 5.0–6.5 mm (because it was not always possible to reconstruct a slice thickness of exactly 5 mm) and a pitch value between 0.75 and 0.85. The results obtained for unit D were similar to those for unit A and have been omitted. The relative error on the SNR measurements is close to 5.0%. The data presented as black squares is for acquisitions with a detector collimation of 5.0 mm. The data presented as white squares is for data acquired with a detector collimation of 2.0–2.5 mm and then reconstructed as 5-mm-thick slices. For a given scanned volume, the use of a detector collimation of 2.0–2.5 mm (instead of 5.0 mm) increases the acquisition time by a factor of 2.5–2.0, respectively, and this setting is called "acquisition without acquisition time constraint". Table 2

Table 1 Normalised $CTDI_w$ for the four units involved in the study

Unit	Measured $nCTDI_{100,w}$ (mGy/mAs)	$nCTDI_{100,w}$ indicated by the unit (mGy/mAs)	Relative difference between measured and indicated $nCTDI_{100,w}$ (%)
A	0.096	0.090	6.4
B	0.073	0.068	7.4
C	0.116	0.105	10.0
D	0.083	0.086	3.6

Fig. 1 a SNR of 5.0-mm-thick reconstructed slices as a function of CTDI$_{vol}$ for unit A. *Black squares* correspond to the acquisitions performed with a detector collimation of 5.0 mm, whereas *white squares* correspond to the acquisitions performed with a detector collimation of 2.5 mm using systematically a pitch of 0.75. **b** Wiener spectrum of 5.0-mm-thick slices obtained with unit A using a pitch of 0.75 and detector collimations of 2.5 mm and 5.0 mm. Similar results were obtained for unit D. **c** SNR of 5.0-mm-thick reconstructed slices as a function of CTDI$_{vol}$. *Black circles* correspond to the acquisitions performed using a detector collimation of 5.0 mm and a pitch of 0.75. *White circles* correspond to the acquisitions performed with a detector collimation of 2.5 mm and a pitch of 1.5
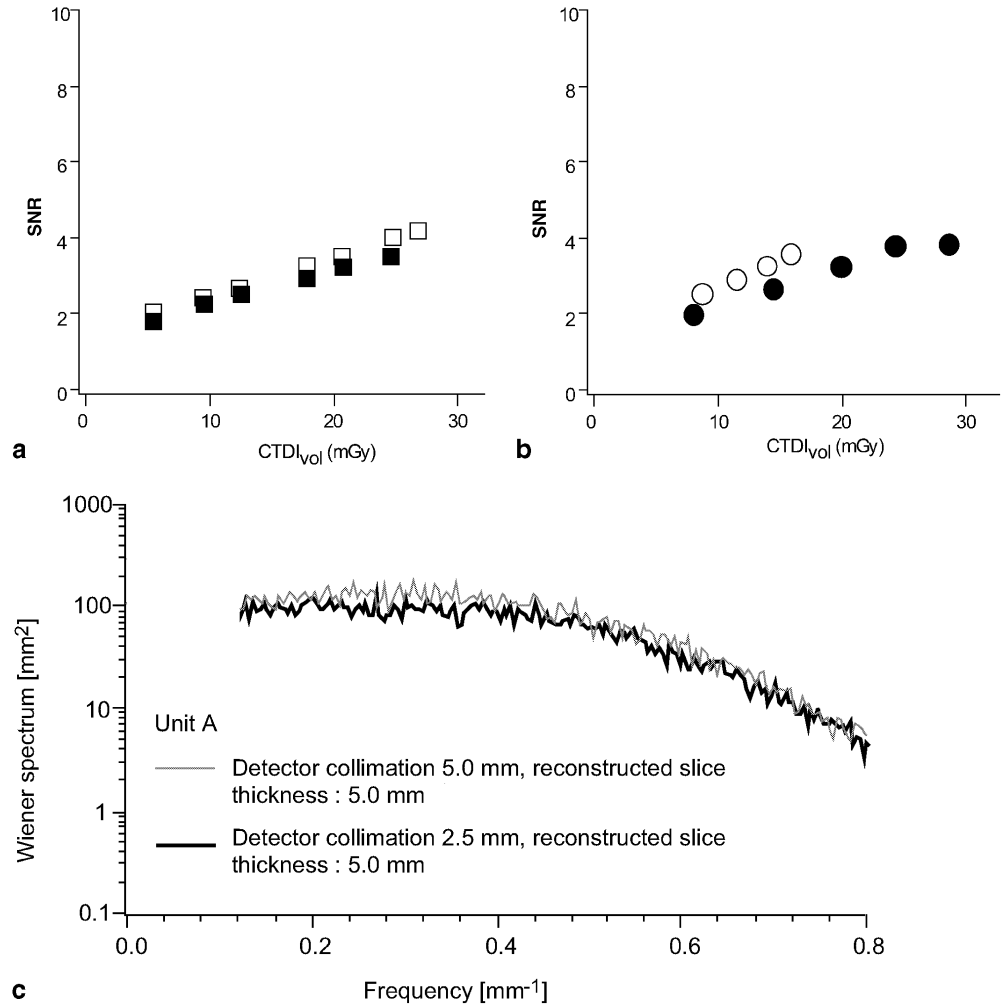

Table 2 FWHM of the SSP measured using a pitch of 0.75–0.85 at various detector collimations using a reconstructed slice thickness of 5.0 mm

Unit	Detector collimation of 2.0–2.5 mm (mm)	Detector collimation of 5.0 mm (mm)
A	5.0±0.1	5.1±0.1
B	5.0±0.1	6.5±0.1
C	5.0±0.1	5.0±0.1
D	5.0±0.1	6.0±0.1

Table 3 Analysis of the data presented in Fig. 1: Student's *t*-test results for acquisitions performed with a pitch of 0.75–0.85. Parameters set 1 (PS1) corresponds to the use of a detector collimation of 2.0–2.5 mm, whereas Parameters set 2 (PS2) corresponds to the use of a detector collimation of 5.0 mm

Unit	Student's *t*-test result	$P<0.05$	Statistical differences between parameter sets 1 and 2
A	2.620	2.306	Yes: PS1 superior PS2
B	0.646	2.447	No: PS1 equal PS2
C	8.680	2.776	Yes: PS1 inferior to PS2
D	2.464	2.776	No: PS1 equal PS2

shows the measured SSPs. The measured and nominal values agree within ±0.1 mm.

Table 3 shows the results of the Student's *t*-test ($P<0.05$) on the SNR measurements obtained without acquisition time constraint. At equivalent CTDI$_{vol}$ values, there is no statistical difference in the SNR between the use of a 2.5- or 5.0-mm detector collimation for units B and D. For unit A, the use of a 2.5-mm detector collimation to get 5-mm-thick slices increases the SNR, and for unit C the use of a 2.0-mm detector collimation to get 5-mm-thick slices significantly decreases the SNR. It is interesting to observe the effect of detector collimation on the longitudinal resolution of the acquisitions; the use of a 5.0-mm detector collimation on the units B and D gives a FWHM of the SSP of 6.5 and 6.0 mm, respectively. The use of a 2.5-mm detector collimation to provide 5-mm slices was only beneficial for unit A.

Fig. 2 **a** SNR of 5.0- and 6.5-mm-thick reconstructed slices as a function of CTDI$_{vol}$ for unit B. *Black squares* correspond to the acquisitions performed with a detector collimation of 5.0 mm (leading to a reconstructed slice thickness of 6.5 mm), whereas *white squares* correspond to the acquisitions performed with a detector collimation of 2.5 mm (leading to a reconstructed slice thickness of 5.0 mm) using systematically a pitch of 0.875. **b** Wiener spectrum of 5.0- or 6.5-mm-thick slices obtained with unit B using a pitch of 0.875 and detector collimations of 2.5 and 5.0 mm. **c** SNR of 5.0- and 6.5-mm-thick reconstructed slices as a function of CTDI$_{vol}$. *Black circles* correspond to the acquisitions performed using a detector collimation of 5.0 mm and a pitch of 0.875. *White circles* correspond to the acquisitions performed with a detector collimation of 2.5 mm and a pitch of 1.25
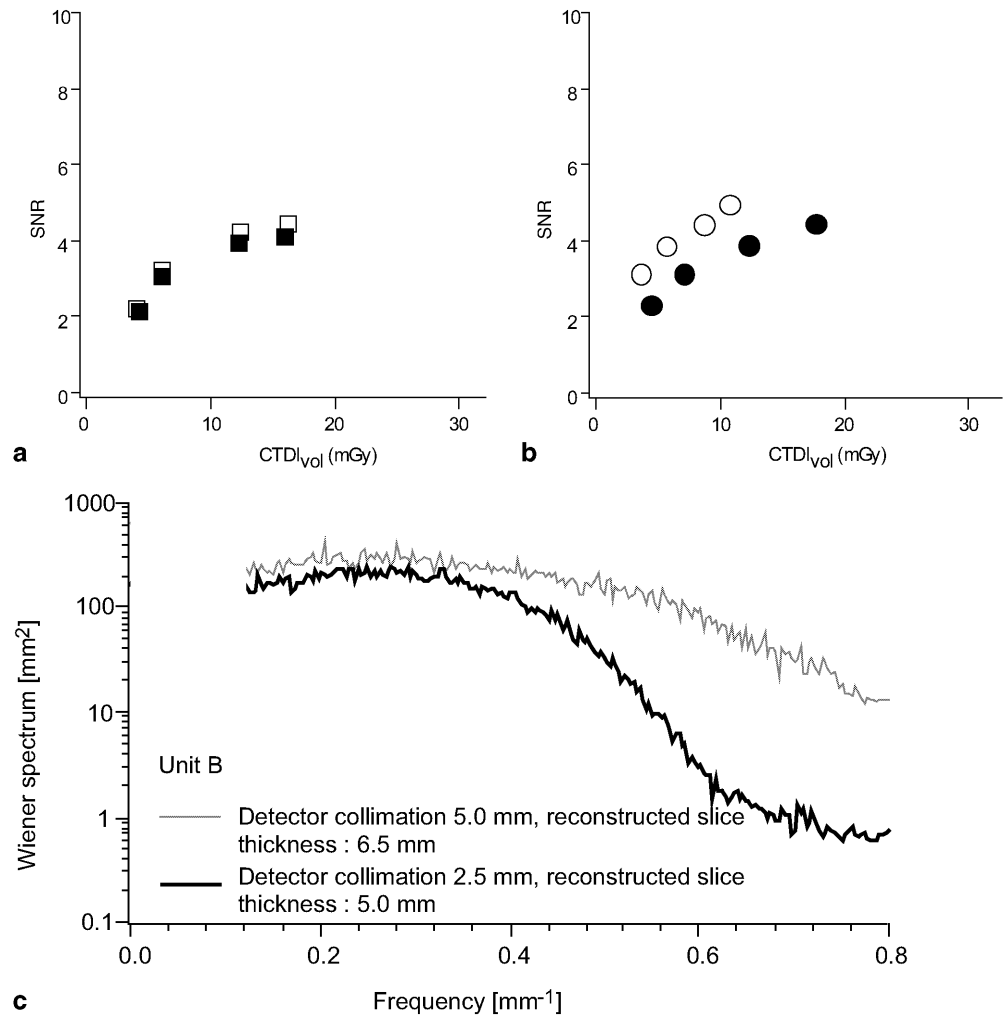
The data shown in Figs. 1a, 2a, 3a were obtained using the filters usually used in the different centres for routine standard abdominal acquisitions. Since SNR measurements do not take into account the spatial frequency content of the noise, these figures should not be used to rank the different units in terms of dose efficiency to reduce image noise.

Figures 1b, 2b, 3b show the Wiener spectra of the image noise for each unit, with a pitch value in the range of 0.75–0.85. Unit D has been omitted since it is similar to unit A. The low frequency range is not represented because the length of the sample used to perform the calculations is too small to provide adequate precision in this range, and because it is not relevant for this study. For units A and D, Fig. 1b shows that a similar filter is used to reconstruct data that are acquired with a detector collimation of 2.5 or 5.0 mm. For unit B (Fig. 2b), the filter applied to reconstruct a 5.0-mm-thick slice is different depending on whether a detector collimation of 2.5 or 5 mm is used. The data are significantly more low-pass filtered

(smoothed) when a detector collimation of 2.5 mm is used than when a detector collimation of 5.0 mm is used. For unit C (Fig. 3b), as for units A and D, there is no change in filter when switching from a detector collimation of 2.0 to 5.0 mm. Nevertheless, the data are highly low-pass filtered when compared with the data in Fig. 1b, 2b.

Figures 1c, 2c, 3c show the variation in SNR as a function of the CTDI$_{vol}$ for a reconstructed slice thickness close to 5.0 mm, for a pitch value of 0.75–0.85 combined with a detector collimation of 5.0 mm, and a pitch value of 1.25–1.5 combined with a detector collimation of 2.0–2.5 mm. The data plotted as black circles are for the acquisitions with a detector collimation of 5.0 mm. The data plotted as white circles are for the acquisitions with a detector collimation of 2.0–2.5 mm, reconstructed as 5-mm-thick slices. For this data, the acquisition duration for a given scan length is comparable, and this setting is called "acquisition with acquisition time constraint".

The SSPs measured for the acquisitions with a detector collimation of 2.0–2.5 mm and a pitch in the range

Fig. 3 a SNR of 5.0-mm-thick reconstructed slices as a function of CTDI$_{vol}$ for unit C. *Black squares* correspond to the acquisitions performed with a detector collimation of 5.0 mm, whereas *white squares* correspond to the acquisitions performed with a detector collimation of 2.0 mm using systematically a pitch of 0.75. **b** Wiener spectrum of 5.0-mm-thick slices obtained with unit C using a pitch of 0.75 and detector collimations of 2.0 and 5.0 mm. **c** SNR of 5.0-mm-thick reconstructed slices as a function of CTDI$_{vol}$. *Black circles* correspond to the acquisitions performed using a detector collimation of 5.0 mm and a pitch of 0.75. *White circles* correspond to the acquisitions performed with a detector collimation of 2.0 mm and a pitch of 1.5
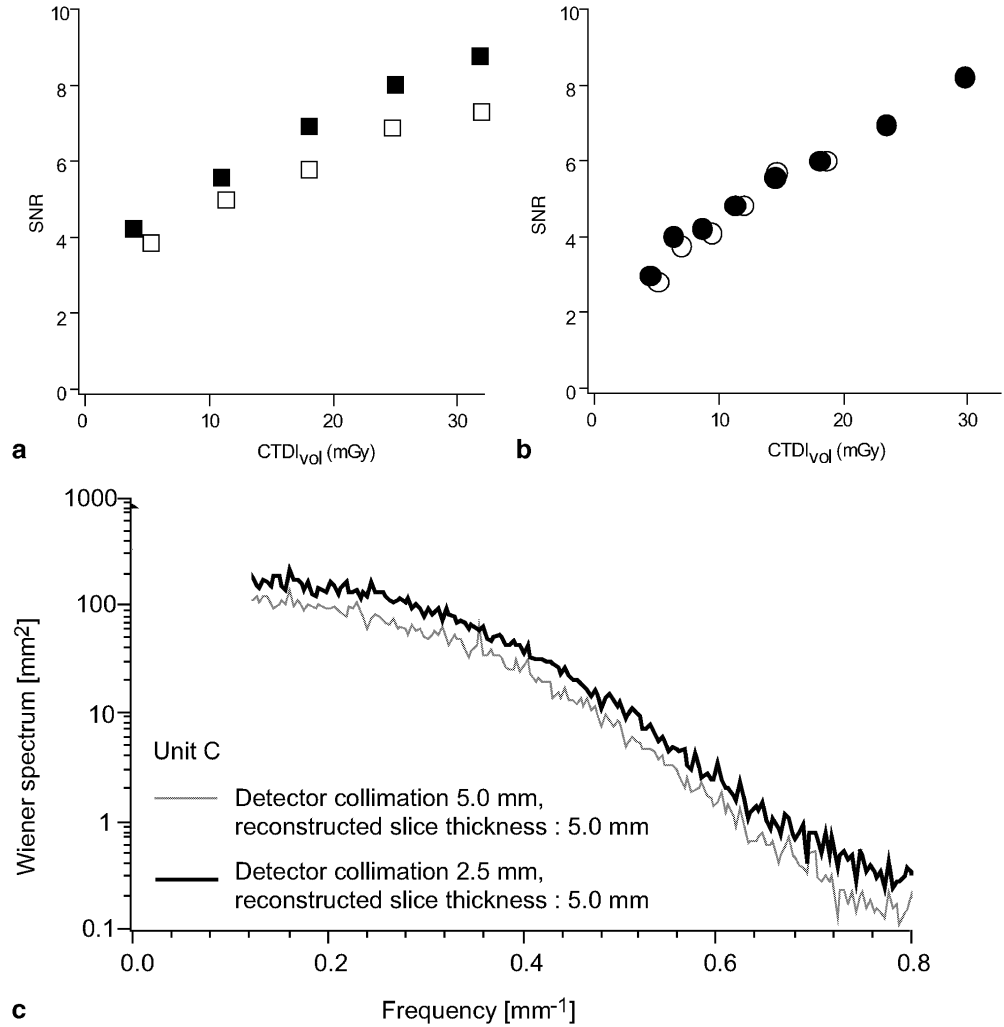

Table 4 Analysis of the data presented in Fig. 6: Student's *t*-test results for acquisitions performed with a pitch of 1.25–1.5 with a detector collimation of 2.0–2.5 mm (PS3) and with a pitch of 0.75–0.85 with a detector collimation of 5.0 mm (PS2)

Unit	Student's *t*-test result	*P*<0.05	Statistical differences between parameter sets 2 and 3
A	5.391	2.306	Yes: PS3 superior PS2
B	8.569	2.447	Yes: PS3 superior PS2
C	2.235	4.303	No: PS3 equal PS2
D	1.302	2.306	No: PS3 equal PS2

1.25–1.5 are similar to those reported in the second column of Table 2. Thus, the use of a pitch value greater than unity, combined with a small detector collimation, allows a good control of the SSP parameter. For all the units, the Wiener spectra obtained with a detector collimation of 2.0–2.5 mm and a pitch in the range 1.25–1.5 are similar to those obtained with a detector collimation of 2.0–2.5 mm and a pitch of 0.75–0.85.

Table 4 shows the results of the Student's *t*-test (*P*<0.05) applied to the SNR measurements obtained with the acquisition time constraint. For units A and B, at a given CTDI$_{vol}$, the use of a detector collimation of 2.5 mm combined with a pitch value of 1.25–1.5 gives a higher SNR than the use of a detector collimation of 5.0 mm and a pitch value of 0.75–0.85. For units C and D, no statistical difference in the SNR is observed between the two sets of acquisition parameters.

Discussion

As expected, there are noticeable differences in the $_n$CTDI$_w$ between the units. These differences are due to the manufacturers' choices for X-ray beam filtering and gantry geometries. The $_n$CTDI$_w$ alone does not indicate whether a particular unit delivers more patient dose than another. It is more appropriate to differentiate the units on the basis of the image quality obtained for a given

CTDI$_w$ for incremental acquisitions, or CTDI$_{vol}$ for helical acquisitions.

There is good agreement between the nominal and measured reconstructed slice thickness (Table 2). For units B and D, in spite of the fact that a detector collimation of 5.0 mm is available from the detector characteristics [detector length in the z-direction: 5 mm; (2.5+1.5+1 mm); (1+1.5+2.5 mm); 5 mm], no SSP of 5.0 mm is available when a detector collimation of 5.0 mm is used. This is, however, possible with units A and C. For all the units, the use of a detector collimation of 2.0 or 2.5 mm allows the reconstruction of a 5.0-mm-slice thickness for any pitch value chosen (0.75–0.85 or 1.25–1.5).

The data presented in Table 3 show that z-filtering of the data does not always lead to an SNR improvement. The statistical analysis of the data shows that, of the four units studied, the use of a smaller detector collimation than the reconstructed slice thickness was beneficial for one unit (A), had no effect on two units (B and D) and was detrimental for one unit (C), for a pitch value slightly less than unity for all the acquisitions. The detrimental effect observed for unit C might be explained by the fact that the 2.0-mm detector collimation used for this particular unit involves smaller detector cells than the other units. The use of small detector cells improves the longitudinal resolution of the acquisitions, but may reduce the efficiency of the conversion of the detected X-ray photons into signal. This behaviour should be carefully monitored, since reductions in the size of detector cells is a trend currently being pursued by manufacturers.

When Fig. 1a or 2a is compared with Fig. 3a, it seems that unit C performs better than the other units in terms of patient dose efficacy (i.e., gives a higher SNR than the other units for a given CTDI$_{vol}$). This may be deceptive, since the SNR evaluation does not take into account the spatial frequency content of the image. In order to assess whether the filters applied to the data were comparable, Wiener spectra of the data were calculated. This allows the variance of the noise to be decomposed into spatial frequency components in order to verify if the data were low-pass filtered in different ways. Several behaviours were observed: for three of the four units, the filter used with a detector collimation of 2.0–2.5 mm and 5.0 mm was the same (units A, C and D); for the fourth unit (unit B), the manufacturer has increased the filtering of the

data when a detector collimation of 2.5 mm rather than 5.0 mm is selected. Comparing Fig. 1 and 3 shows that images produced on unit C are significantly more low-pass filtered than images produced on unit A. Note that, for the in-plane spatial resolution, the pixel size chosen during the acquisitions gives a Nyquist frequency of 0.71 mm^{-1} [i.e., (1/2) × pixel size, which is 0.7 mm]—and so the different strategies adopted by manufacturers for data filtering might have an impact on in-plane resolution. The type of filtering used on unit C might be better than that used on unit A when dealing with the detection of large low contrast structures, but may give less information than unit A when dealing with the detection of small high contrast structures.

The results obtained with a higher pitch value (to maintain comparable acquisition duration) and a small detector collimation or a 5.0-mm detector collimation are also unit dependent. For units A and B, it is better, in terms of SNR, to use a detector collimation of 2.5 mm and a pitch of 1.25 or 1.5 to get a 5.0-mm-slice thickness than to use a detector collimation of 5.0 mm with a pitch of 0.75 or 0.85. However, it must be noted that a higher filtering is applied to the data for unit B when the 2.5-mm detector collimation is used.

Conclusion

From the results presented in this study, it appears that no general conclusions can be drawn concerning the superiority of the use of a smaller detector collimation than the reconstruction slice thickness for SNR. Moreover, this study has shown the limitations of SNR calculations based on a standard deviation calculation for evaluating the performances of different CT units. Such an approach is, however, convenient when the aim of the study is restricted to patient dose optimization on a particular system [15]. To fully understand the behaviour of the noise variations, the Wiener spectra should be evaluated to take into account the reconstruction kernel used during the processing of the data.

References

1. Kalender WA, Seissler W, Klotz E, Vock P (1990) Spiral volumetric CT with single-breath-hold technique, continuous transport, and continuous scanner rotation. Radiology 176:181–183

2. Liang Y, Kruger RA (1996) Dual-slice spiral versus single-slice spiral scanning: comparison of the physical performance of two computed tomography scanners. Med Phys 23:205–220

3. Hu H, He HD, Foley WD, Fox SH (2000) Four multidetector-row helical CT: image quality and volume coverage speed. Radiology 215:55–62

4. McCollough CH, Zink FE (1999) Performance evaluation of a multi-slice CT system. Med Phys 26:2223–2230

5. Hu H, Fox SH (1996) The effect of helical pitch and beam collimation on the lesion contrast and slice profile in helical CT imaging. Med Phys 23:1943–1954

6. Brooks RA, Di Chiro G (1976) Statistical limitations in X-ray reconstructive tomography. Med Phys 3:237–240
7. Kalender WA, Schmidt B (2000) Recent advances in CT: will doses go down or will they go up? Physica Medica 16:137–144
8. Hu H, Shen Y (1998) Helical CT reconstruction with longitudinal filtration. Med Phys 25:2130–2138
9. Hu H (1999) Multi-slice helical CT: scan and reconstruction. Med Phys 26:5–18
10. Shin HO, Falck CV, Galanski M (2004) Low-contrast detectability in volume rendering: a phantom study on multidetector-row spiral CT data. Eur Radiol 14(2):341–349
11. International Electrotechnical Committee (1994) Medical diagnostic X-ray equipment—radiation conditions for use in the determination of characteristics. Standard IEC #61267, Geneva
12. International Electrotechnical Committee (1999) Medical diagnostic X-ray equipment—particular requirements for the safety of X-ray equipment for CT 1999. Standard IEC #60601-2-44, Geneva
13. International Electrotechnical Committee (2002) Medical diagnostic X-ray equipment—particular requirements for the safety of X-ray equipment for CT. Standard IEC #60601-2-44, Geneva
14. Dainty JC, Shaw R (1974) Image science. Academic, London
15. Greess H, Lutze J, Nomayr A, Wolf H, Hothorn T, Kalender WA, Bautz W (2004) Dose reduction in subsecond multislice CT examination of children by online tube current modulation. Eur Radiol 14(6):995–999